Unfolding of *trp* Repressor Studied Using Fluorescence Spectroscopic Techniques†

Teresa Fernando‡ and Catherine A. Royer*,§

School of Pharmacy, University of Wisconsin, Madison, Wisconsin 53706, and Department of Biochemistry, University of Illinois, Urbana, Illinois 61801

Received January 15, 1992; Revised Manuscript Received April 28, 1992

ABSTRACT: The unfolding properties of the *trp* repressor of *Escherichia coli* have been studied using a number of different time-resolved and steady-state fluorescence approaches. Denaturation by urea was monitored by the average fluorescence emission energy of the intrinsic tryptophan residues of the repressor. These data were consistent with a two-state transition from dimer to unfolded monomer with a free energy of unfolding of 19.2 kcal/mol. The frequency response profiles of the fluorescence emission brought to light subtle urea-induced modifications of the intrinsic tryptophan decay parameters both preceding and following the main unfolding transition. The increase in lifetime induced by urea required higher concentrations of urea than the increase in the total intensity described by Gittelman and Matthews [(1990) *Biochemistry 29*, 7011]. This indicates that the intensity increase has both dynamic and static origins. To assess the effect of tryptophan binding upon repressor stability, and to determine whether repressor oligomerization would be detectable in an unfolding experiment, we examined denaturation profiles of repressor labeled with the long-lived fluorescence probe 5-(dimethylamino)naphthalene-1-sulfonyl (DNS), by monitoring the average rotational correlation time of the probe. These experiments revealed a protein concentration dependent transition at low urea concentrations. This transition was promoted by tryptophan binding. We ascribe this transition to urea-induced dissociation of repressor tetramers. The main unfolding transition of the dimer to unfolded monomer was also observable using this technique, and the free energies associated with this transition were 18.3 kcal/mol in the absence of tryptophan and 24.1 kcal/mol in its presence, demonstrating that co-repressor binding stabilizes the repressor dimer against denaturation. In summary, the unfolding of the repressor dimer is largely a two-state phenomenon, although it is preceded by the dissociation of repressor tetramers, and may also involve a continual effect of urea on the denatured state.

The *trp* repressor of *Escherichia coli* (TR)[1] is a regulatory protein involved in modulating the transcriptional levels of the genes whose products are responsible for tryptophan biosynthesis. In the presence of external tryptophan, the bacteria have no need to synthesize these proteins, and thus, the *trp* repressor, when bound by tryptophan, occupies an operator sequence within the *trp* EDCBA promoter region, thereby inhibiting the binding of RNA polymerase and repressing synthesis of the downstream genes. The specific protein–DNA complex has been shown to involve the dimeric tryptophan-bound form of the 12 600 molecular weight *trp* repressor polypeptide (Otwinowski et al., 1988; Carey, 1988). However, we have recently demonstrated that this protein can exist in a number of oligomeric states depending upon the concentration of protein, tryptophan, and DNA (Fernando & Royer, 1992). The binding of multiple dimers of *trp* repressor to specific and nonspecific DNA has been observed by other investigators (Kumamoto et al., 1987; Carey, 1988; Staake et al., 1990). In our previous work, we demonstrated that the binding of tryptophan by the repressor leads to the destabilization of the tetrameric and any higher order oligomeric species toward the active, dimeric form of the protein. Because the ligand makes contact with each of the two monomeric subunits in the dimer (Schevitz et al., 1985), we also expected that tryptophan binding would stabilize the dimer with respect to monomeric repressor. From dilution data in our previous work, we estimated a monomer–dimer dissociation constant for the aporepressor of less than 1 nM. Due to this relatively high affinity, we were unable to fully characterize that transition thermodynamically, and the technique used, dilution profiles of the protein's intrinsic fluorescence, precluded studying the effect of tryptophan upon the monomer–dimer equilibrium.

In order to test whether, in fact, ligation by tryptophan stabilizes the interaction between repressor monomers, we opted to study the effect of tryptophan binding on the denaturation profiles of the repressor. As in our previous dilution studies, the protein was covalently modified by a fluorescent dye whose absorption and emission spectra are of much lower energy than those of the intrinsic protein fluorescence and the tryptophan ligand. The dye 5-(dimethylamino)naphthalene-1-sulfonyl chloride (DNS) has an absorption maximum near 350 nm and an emission maximum near 500 nm. In this manner, denaturation profiles of the repressor in the absence and presence of tryptophan were generated by measuring the anisotropy and lifetime of fluorescence of the DNS label as a function of urea concentration. These values allow for the calculation of the average rotational correlation time of the probe, which is a result of depolarization by both the global tumbling of the macromolecule and the local motions of the DNS probe. As the protein oligomer dissociates and unfolds, the correlation time is expected to decrease due to the decrease in size of the macromolecule upon dissociation as well as the increased flexibility of the DNS probe in the unfolded state.

Lane and Jardetsky (1987) and Gittelman and Matthews (1990) used the intrinsic tryptophan emission, among other

† Supported by a grant to C.A.R. from the National Institutes of Health (R-29-GM39969).

* To whom correspondence should be addressed.

‡ University of Illinois.

§ University of Wisconsin.

[1] Abbreviations: TR, *trp* repressor; DNS, 5-(dimethylamino)naphthalene-1-sulfonyl moiety; TR-DNS, DNS-labeled *trp* repressor; W19, tryptophan-19; W99, tryptophan-99.

0006-2960/92/0431-6683$03.00/0

techniques, to monitor *trp* repressor unfolding. The first group, by differentiating between the red and the blue edge of the emission spectrum using iodide quenching as a function of urea concentration, concluded that the transition from folded to unfolded protein involved intermediate species at equilibrium. On the other hand, the second group, monitoring the intensity above 325 nm, concluded that the transition was two-state. Neither group saw evidence for higher order oligomers of the repressor, although they worked at concentrations where these species are significantly populated. In our previous study on the oligomerization properties of the repressor, we demonstrated that the intrinsic tryptophan emission intensity and energy were insensitive to the formation of the higher order oligomers. Since the anisotropy of the fluorescence of the DNS label is quite sensitive to the size of the protein, whereas the tryptophan emission intensity is not, we expected that the DNS label would be a better reporter than the intrinsic tryptophan emission as to whether the transition from tetramer to unfolded monomer would be concerted, or whether the dimeric intermediate would be observed.

In addition to monitoring the fluorescence properties of the DNS-labeled repressor, we have also undertaken the study of the steady-state emission energy and the nanosecond decay of the intrinsic tryptophan fluorescence in an attempt to observe and characterize any intermediates, such as those reported by Lane and Jardetsky (1987). To this end, the lifetimes of the intrinsic tryptophan residues (W19 and W99) were studied at multiple emission wavelengths and urea concentrations. W19, on the amino-terminal part of the protein in helix A, is found at the interface between the two monomeric subunits, whereas W99, on the carboxy-terminal F helix, is more exposed to solvent (Zhang et al., 1987). This section of the F helix is positioned on top of the central core of the protein made up of interlocking ABC helices from both subunits. One would expect then that in the native protein, the emission spectrum of W99 would be red-shifted, due to greater exposure to solvent, with respect to the emission of W19, which is buried at the subunit interface. In our previous work, we demonstrated that they could be partially resolved by a multiwavelength time-resolved study of the fluorescence quenching by potassium iodide. We ascribed a blue, 3–4-ns lifetime component to emission from W19 and a red, short component (near 0.5 ns) to emission from W99. An intermediate lifetime component appeared to account for emission heterogeneity from both residues. Carey and co-workers (personal communication) using chymotryptic fragments of the protein containing either the ABC helix sequences or the DEF sequences demonstrated that the ABC fragment folds into a stable dimer and that it exhibits approximately 90% of the fluorescence intensity of the native protein. The unfolded DEF fragment has a spectrum quite similar to the unfolded native protein, in emission maximum, but exhibits a higher total intensity. With this partial discrimination of the two tryptophan residues, we reasoned that if intermediates are involved in the equilibrium unfolding of the protein, the denaturation profiles which would be generated if one could observe separately the emission parameters (intensity, color, lifetime) of these tryptophan residues may not be identical. Although the complete separation of the emission of the two residues is only possible using single-tryptophan mutants of the repressor, the time resolution of the emission as a function of wavelength and urea concentration might allow for the discrimination of the unfolding of the central core (W19) as opposed to the outer surface (W99) of the protein.

MATERIALS AND METHODS

Protein Purification. *Trp* repressor either was a gift from Dr. K. S. Matthews or was purified in our laboratory. In either case, it was purified from the overproducing strain CY15071 and transformed with the PJPR2 plasmid containing the gene for the repressor. The protein was purified following the procedures described by Paluh and Yanofsky (1986), with modifications as described by He and Matthews (1989). The repressor preparations were tested for operator DNA binding following the method described by Carey (1988) using a 40 base pair oligonucleotide containing the *trp* EDCBA operator sequence described by Chou et al. (1990) and were found to bind with a K_d of 0.5 nM. The purity of the samples as assessed by silver stain of SDS–PAGE was greater than 95%.

DNS Labeling. *Trp* repressor solutions (1 mL) at concentrations of 3–18 mg/mL were dialyzed against 1 L of 240 mM potassium phosphate buffer at pH 8 for 3 h at 4 °C. After dialysis, 10–20 μL of a 0.02 M solution of dansyl chloride [5-(dimethylamino)naphthalene-1-sulfonyl chloride] purchased from Molecular Probes (Eugene, OR) was added, and the labeling reaction was allowed to proceed for approximately 10 min. The solution was then applied to a Sephadex G-25 superfine desalting column, and the labeled protein was recuperated in the void volume. This solution was then dialyzed against 10 mM phosphate, pH 7.6, for 24 h before experiments were carried out. The concentration of dye was calculated from the absorption at 350 nm assuming an extinction coefficient of 4500 cm^{-1} M^{-1}. That of the protein was calculated by the method of Jameson (1975). Labeling ratios were typically between 0.5 and 1 mol of dye per/mol of dimer. Urea was Ultrapure purchased from ICN Biomedicals (Costa Mesa, CA).

Steady-State Fluorescence Measurements. Steady-state anisotropy measurements of the DNS-labeled repressor were carried out exciting at 340 nm and monitoring the emission at 500 nm with a monochromator in place using a bandwidth of 16 nm, or with no monochromator but a cuton emission filter, Y460 (Hoya Optics, Sunnyvale, CA). The anisotropy, A, was calculated from the parallel and perpendicular emission components as

$$A = (I_{\parallel} - I_{\perp})/(I_{\parallel} + 2I_{\perp}) \quad (1)$$

Measurements were averaged until the error was ±0.004. Steady-state emission spectra of the intrinsic tryptophan fluorescence were acquired with an excitation wavelength of 295 nm, and the emission was scanned from 310 to 450 nm with an 8-nm band-pass in both excitation and emission. All measuements were performed on either an ISS Greg PC or an ISS KOALA (ISS, Inc., Urbana, IL). The average emission energy, $\bar{\nu}_g$, was calculated using the ISS spectral software as

$$\bar{\nu}_g = \sum_i (F_i \nu_i)/\sum_i F_i \quad (2)$$

where ν_i is the emission energy in wavenumbers and F_i is the corresponding intensity. All spectra were corrected for the background fluorescence of urea containing buffer at the same concentration as the sample.

Time-Resolved Fluorescence Measurements. The fluorescence lifetimes of the intrinsic tryptophan emission were measured using the cavity-dumped frequency-doubled output of an R6G dye laser 700 series pumped with the mode-locked frequency-doubled output of an Antares Nd-YAG laser (all components from Coherent Corp., Palo Alto, CA). Data collection was in the frequency domain using an ISS KOALA

and frequency domain electronics. Frequency response curves were analyzed for lifetime and preexponential values with the global analysis software Globals Unlimited (LFD, Urbana, IL) which is described in detail elsewhere (Beechem et al., 1992).

Lifetimes of the DNS label were obtained using the acousto–optically modulated 325-nm line of a CW helium neon laser from Liconix, Inc., as described by Piston et al. (1990). Average lifetime values were calculated as the weighted average of the recovered components using the recovered fractional intensity values. These were used with the steady-state anisotropy values to calculate an average rotational correlation time, τ_c, as follows:

$$A_0/A - 1 = \langle\tau\rangle/\langle\tau_c\rangle \quad (3)$$

Unfolding Data Analysis. The unfolding profiles obtained using either intrinsic tryptophan emission energy or DNS anisotropy values were directly fit using a nonlinear least-squares analysis routine derived from the global analysis binding software described by Royer et al. (1990) assuming a two-state transition from dimer to unfolded monomer. The experimental observable (either τ_c, correlation time, or $\bar{\nu}_g$, emission energy) was mapped directly to the fraction of unfolded monomer, assuming that this species was 100% populated at the high urea concentration plateau and 0% populated in the absence of urea. The plateau values of the observables were variable parameters in the fits. The data were fit in terms of the free energy of the dissociation/unfolding transition and its cooperativity. The free energy of unfolding is taken to vary linearly with the concentration of urea (Pace, 1986), with an intercept corresponding to the free energy of unfolding in the absence of urea and a slope which is dependent upon the degree of cooperativity of the unfolding transition:

$$\Delta G_i = \Delta G_0 + A[\text{urea}] \quad (4)$$

where ΔG_i, the free energy of unfolding at each urea concentration, is calculated from the equilibrium constant, K_i, at that same concentration as

$$\Delta G_i = -RT \ln K_i \quad (5)$$

All free energies are reported in units of kilocalories per mole.

RESULTS

Intrinsic Tryptophan Fluorescence Denaturation Profiles. The intrinsic tryptophan emission of the *trp* repressor arises from residues 19 and 99. From time-resolved fluorescence iodide quenching data (Fernando & Royer, 1992), we have proposed that in the native protein, the emission arises predominantly from W19, which is buried at the interface between the two monomeric subunits. Carey (personal communication) has shown that the fragment of the protein containing the ABC helices (and thus W19), which forms a folded dimeric structure in solution, exhibits a fluorescence signal quite similar in total intensity and energy to the wild-type protein. Lane and Jardetsky (1987) and Gittelman and Matthews (1990) report an increase in the intrinsic fluorescence intensity of the repressor as the concentration of urea is increased. We too have observed an increase in the steady-state fluorescence intensity as a function of urea concentration. The steady-state emission spectra of 2 μM *trp* repressor dimer between 0 and 9 M urea are shown in Figure 1a. The spectrum of the native protein is rather blue. As the concentration of urea is increased, the emission maximum shifts to the red. In addition, the total intensity of the spectrum increases. In other words, there is a loss of intensity on the blue edge of the spectrum, which is recovered on the red edge, but also the intensity on the red edge increases beyond the peak value of the native spectrum. We interpret these changes in terms of both a shift to the red of tryptophan-19 as the interface between the monomeric subunits is disrupted and also an increase in the fluorescence of tryptophan-99 as the quenching is lifted by the loss of the secondary structure in the DEF helices. The average emission energy of each spectrum was calculated as described under Materials and Methods. This quantity is an integral quantity and is much less subject to random noise than the value of the emission maximum. The plot of the average emission energy as a function of urea concentration for three concentrations of repressor expressed in terms of dimer can be found in Figure 1B. These data were fit globally to a dimer to unfolded monomer model as described under Materials and Methods, linking the free energy value across data sets. The emission energy served as the experimental observable used to calculate the apparent fraction unfolded. The free energy of unfolding from dimer to unfolded monomer recovered from the fit was 19.2 kcal/mol, which is slightly lower than the free energy reported by Gittelman and Matthews (1990), 22 kcal/mol. The global χ^2 value for the fit was 0.93. Rigorous confidence limit testing revealed a well-defined χ^2 minimum, with the 67% confidence limit corresponding to +1.2/–0.9 kcal/mol. The midpoint of the curve for 2 μM was near 5.5 M urea. A summary of the results can be found in Table I.

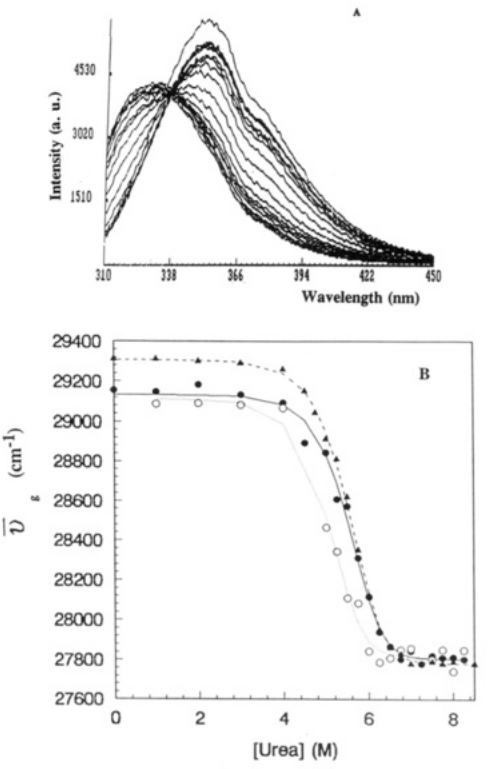

FIGURE 1: (A) Emission spectra of *trp* repressor between 0 and 9 M urea. Spectra are corrected for background fluorescence from the buffer or urea. (B) Average emission energy of the spectra in (A) plotted as a function of the urea concentration (▲), 2 μM in dimer, and also data collected for (●) 5 μM and (○) 0.5 μM in dimer. Data sets were analyzed globally, linking the free energy of denaturation across the three data sets. The global χ^2 value was 0.92.

The denaturation profile obtained from the emission energy was apparently reflecting very clear-cut two-state unfolding behavior. The total intensity, however, showed more complex patterns. Although above 7 M urea the intrinsic energy (color)

Table I: Results of Analysis of *trp* Repressor Denaturation Profiles[a]

sample	observable	ΔG_0 (kcal/mol)	slope	χ^2
TR	$\bar{\nu}_g$	19.2 ± 1.1	2.12	0.92
TR-DNS	τ_f	18.3 ± 1.5	1.94	1.86
TR-DNS + W	τ_c	24.1 ± 2.6	2.65	1.80

[a] Analysis was carried out in terms of a dimer to unfolded monomer model.

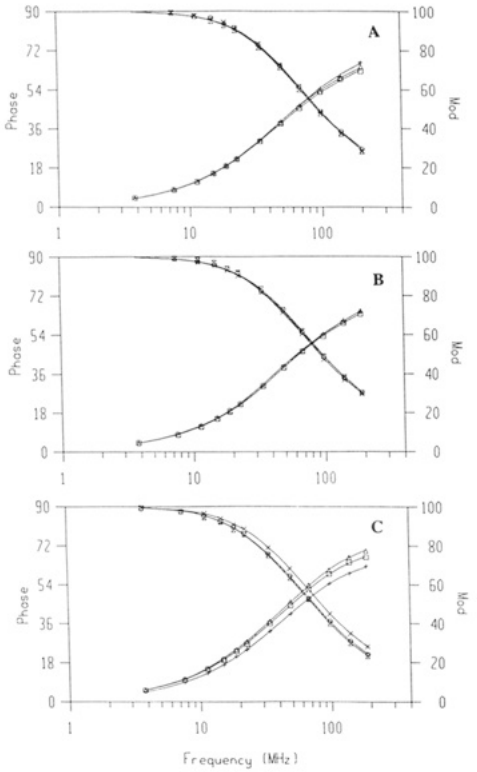

FIGURE 2: Frequency response curves of *trp* repressor (10 μM in dimer) at (A) 0.0, (B) 1.8, and (C) 7.3 M urea. Excitation was at 295 nm and emission was monitored at 320 [(+) phase, (×) modulation], 350 [(□) phase, (○) modulation], and 380 [(△) phase, (△) modulation] nm.

of the emission spectrum exhibits no further changes (Figure 1B), the value of the total intensity continues to rise (Figure 1A). This phenomenon was also observed and reported by Gittelman and Matthews (1990), whose intensity measurements exhibited two slopes, one in the area of the main unfolding transition and a second increase with a larger slope at higher urea concentrations. In order to better understand these changes in intensity, we performed fluorescence lifetime measurements as a function of urea concentration for the aporepressor at a concentration of 10 μM in dimer. The frequency response curves at 320, 350, and 380 nm were measured at nine urea concentrations. Those at 0, 1.8, and 7.3 M are shown in Figure 2A–C. From the raw data, it can be seen that between 0 and 1.8 M urea, the heterogeneity in the emission between the three wavelengths decreases slightly, indicating some type of structural rearrangement is occurring at low urea concentrations, although the changes in tryptophan emission are quite subtle. Above 1.8 M urea, there is a continual increase in the intrinsic fluorescence lifetime, as evidenced by the gradual shift to lower frequency of the frequency response curves, as well as a large increase in the heterogeneity. The data could be analyzed in terms of a triple-exponential decay or a combination of a distribution of lifetimes and a single decay near 500 ps. Regardless of the analysis scheme, χ^2 values were comparable. The increase in the lifetime on the red edge of the spectrum as a function of urea

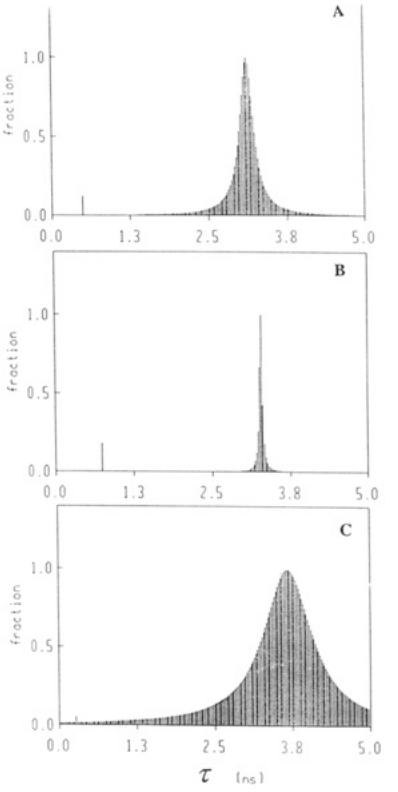

FIGURE 3: Lifetime distribution profiles recovered from analysis of the data obtained at 350 nm in Figure 2. Plots are as follows: (A) 0.0, (B) 1.8, and (C) 7.3 M urea. The global χ^2 values for these analysis were between 0.5 and 2.1. No improvement in χ^2 was obtained when the data were analyzed as a triple-exponential decay, rather than a single exponential and a distributed component.

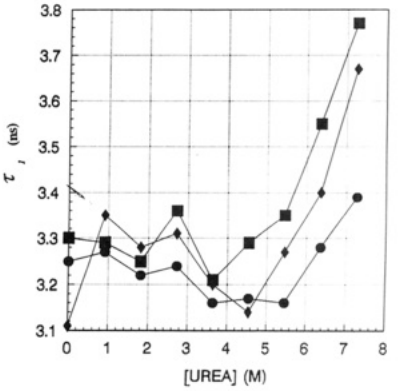

FIGURE 4: Center of the distributions of lifetimes obtained from analysis of the data at 320 (●), 350 (♦), and 380 (■) nm plotted as a function of urea concentration.

concentration was twice as large as that on the blue edge of the spectrum.

When the analysis is carried out in terms of a distribution of lifetimes and a 500-ps discreet component, the changes in the lifetime heterogeneity and the average lifetime value are most easily appreciated. The recovered lifetime distributions obtained from the analysis of the data taken at 350 nm in emission at 0, 1.8, and 7.3 M urea are plotted in Figure 3A–C. The decrease in the heterogeneity of emission at low urea concentrations is evidenced by the decrease in the width of the distribution. At higher urea concentrations, as the protein undergoes the main unfolding transition the width of the distribution again increases, and its center shifts to higher lifetime values. In Figure 4 are plotted the lifetime values of the center of the distribution at 320, 350, and 380 nm as a function of urea concentration. The solution was 20 μM in

repressor monomer. Gittelman and Matthews (1990) demonstrated by circular dichroism that the midpoint of the main unfolding transition is near 5.7–5.8 M urea for 19.4 μM repressor and that the transition is complete by 6.5 M urea for that concentration. They also demonstrated that the unfolding monitored by the fluorescence intensity and that monitored by CD were superimposable if one corrected the fluorescence plots for the slopes preceding and following the main transition. In contrast to the emission energy profile (Figure 1B), the midpoints of the plots of lifetime vs [urea] at all three emission wavelengths are shifted to higher urea concentrations, and the transitions are apparently not complete by 6.5 M urea. These lifetimes results indicate, first of all, that the increase in the total fluorescence intensity observed by Gittelman and Matthews (1990) is at least in part due to a lifting of the dynamic quenching of fluorescence at high urea concentrations. Second, the fact that the total intensity and lifetime profiles are not superimposable in this system indicates that the changes in intensity observed upon unfolding have both static and dynamic origins. The red shift in emission corresponds well to the main unfolding transition and most likely arises from both an increase in intensity of Trp-99 and the red shift of Trp-19 upon unfolding. We interpret the continued increase in intensity and lifetime beyond 6.5 M urea as an effect of high concentrations of urea on the local environment of either one or both of the tryptophan residues, as well as a direct effect of urea on the fluorophore intensity (approximately 4%/M).

TR-DNS Denaturation Profiles. The intrinsic tryptophan emission energy profiles were more consistent than the intensity data of Gittelman and Matthews (1990) with a relatively concerted two-state dimer to unfolded monomer transition, although the lifetime profiles were more complex. We have previously demonstrated that in the absence of any salt, even at concentrations as low as 2 μM in dimer, nonnegligible amounts of repressor tetramer are present in solution (Fernando & Royer, 1992). While no change in the steady-state fluorescence profiles was apparent which could arise from tetramer dissociation, lifetime measurements had brought to light very subtle, but measurable, changes in the decay properties of the tryptophan emission at low urea concentrations. In order to determine if protein oligomer dissociation preceded the main dimer to unfolded monomer transition, anisotropy denaturation profiles using a DNS-labeled repressor were carried out. Due to the red-shifted absorption and emission properties of the DNS probe with respect to tryptophan, these experiments also allowed us to monitor the effect of co-repressor binding on the stability of the repressor. The fluorescence anisotropy of DNS-labeled *trp* repressor (TR-DNS) at a concentration of 2 μM in repressor dimer was measured as a function of increasing urea concentration in the absence and in the presence of 0.4 mM tryptophan. These plots are shown in Figure 5. The anisotropy denaturation profile for the repressor in the absence of tryptophan shows a single transition to lower anisotropy with a midpoint near 6.2 M urea. The profile observed in the presence of tryptophan is biphasic, with one transition between 0 and 2.5 M urea and the second with a midpoint near 6.5 M urea. The anisotropy values in the absence of any urea for the TR-DNS samples in the absence and in the presence of tryptophan are quite similar to those observed at the same concentration in our previous dilution studies. The higher values in the absence of tryptophan are due to the greater percentage of repressor tetramer when no co-repressor is present (Fernando & Royer, 1992).

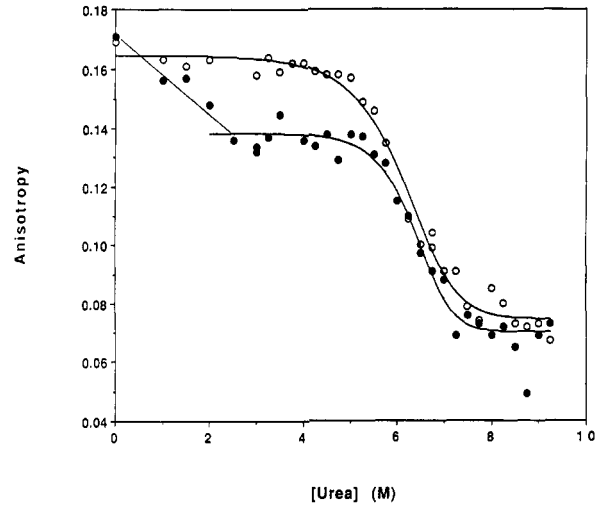

FIGURE 5: Fluorescence anisotropy profiles as a function of urea concentration for DNS-labeled *trp* repressor at 2 μM in dimer in the absence (○) and in the presence (●) of 0.4 mM L-tryptophan. DNS excitation was at 340 nm, and emission was monitored with the monochromator set at 500 nm. The bandwidth was 16 nm in both excitation and emission.

Changes in lifetime values upon denaturation can give rise to observed changes in anisotropy which are not due to any modification of the rotational properties of the probe or protein. For this reason, fluorescence lifetimes for the TR-DNS preparations at 2 μM were also measured as a function of [urea] both in the absence and in the presence of tryptophan. The data were analyzed in terms of a set of three fluorescence lifetimes in each case. For each preparation (±tryptophan), the fluorescence lifetime values were linked across urea concentrations, while the fractional contribution of each lifetime species was allowed to vary between data sets. This analysis is similar to the analysis schemes used for a number of DNS-labeled proteins (Royer et al., 1989, 1990; Guest et al., 1991; Royer & Fernando, 1992). In all cases, the decay fits best to a triple-exponential decay, and in general, these values can be linked across perturbant data sets (salt, pressure, protein concentration, urea) while the preexponential factors are allowed to vary. The complex decay of DNS is related to the exposure to solvent (Royer et al., 1989; Lambooy et al., 1982; Guest et al., 1991). The greater the solvent exposure, the shorter the lifetime and the lower the emission energy. The heterogeneity of the decay in the native protein is assumed to have a dynamic structural origin, resulting in subpopulations of the label on the protein with differing solvent exposure. The fractional intensities for each lifetime component at each urea concentration are plotted in Figure 6A and 6B, respectively, in the absence and in the presence of tryptophan. It can be seen from the plots in Figure 6 that there is a significant decrease in the DNS lifetime between 0 and 4 M urea in the absence of tryptophan but that there is almost no change in the presence of tryptophan over this urea concentration range. Both solutions exhibit a significant decrease in lifetime between 4.5 and 8 M urea, although the change is largest in the absence of tryptophan.

Since changes in the value of the lifetime of the DNS label (τ) can influence the observed anisotropy profile, the average correlation time (τ_c), which is related to the anisotropy (A) as described under Materials and Methods, gives a better measure of changes in the rotational properties of the probe on the protein than the raw anisotropy values and was calculated using eq 3 as described under Materials and Methods. The loss of anisotropy from the limiting value for the probe (A_0) through rotational motion during the excited-

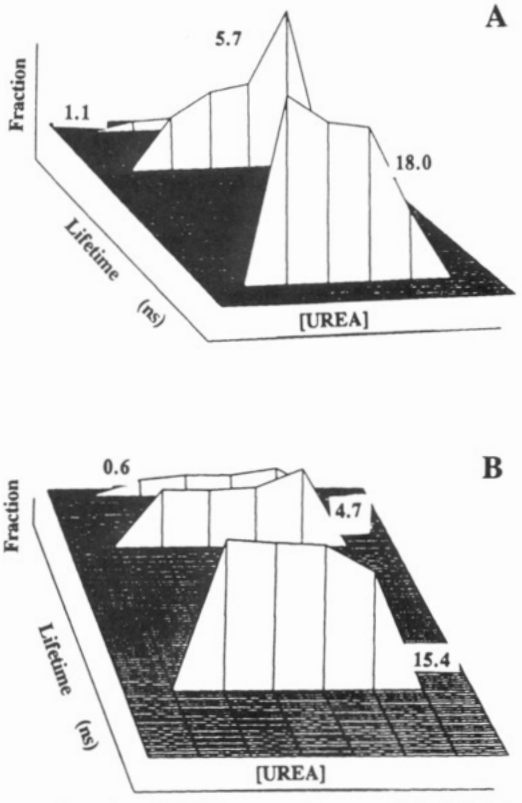

FIGURE 6: Results of lifetime experiments of DNS-labeled *trp* repressor at a dimer concentration of 2 μM as a function of urea concentration. Phase and modulation frequency response curves were obtained at 0, 4.0, 4.5, and 8 M urea. Plots of the fractional contribution to the intensity of each of the recovered lifetime components as a function of urea concentration are shown (A) in the absence of tryptophan and (B) in the presence of 0.4 mM tryptophan. The data were analyzed globally in terms of a consistent set of decay rates among all four data sets (plus or minus tryptophan), and the fractional contribution of each was allowed to vary. The global χ^2 values for these analyses were 2.9 and 3.2, respectively, in the absence and in the presence of tryptophan.

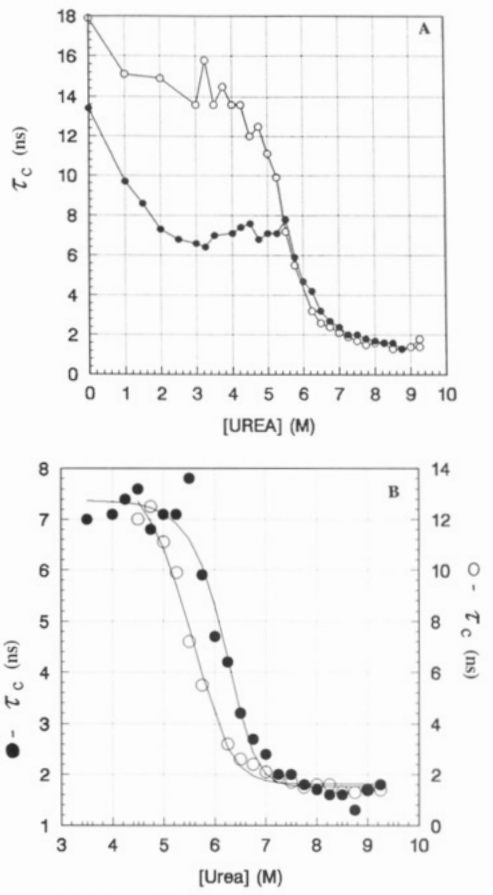

FIGURE 7: Dependence of the average correlation time of the DNS-labeled repressor as a function of urea concentration (A) Plots of average correlation time vs [urea] in the absence (○) and in the presence (●) of 0.4 mM L-tryptophan. (B) To highlight the effect of tryptophan on the main unfolding transition, the average rotational correlation times of the DNS-labeled repressor in the absence (○) and in the presence (●) of tryptophan are plotted to scale. Data are from the main transition in (A) while the lines correspond to the fit calculated from the nonlinear least-squares analysis of the data. The χ^2 values for the two fits were 1.86 and 1.80, respectively, in the absence and in the presence of tryptophan.

state lifetime is related to the tumbling of the macromolecule and the local rotational motion of the probe, while the ability to observe the anisotropy decrease is dependent on the length of time the fluorophore remains in the excited state. Since the DNS lifetime and intensity changes occurred over the same range, the values of the average lifetime at all the concentrations where anisotropy was measured were estimated from the total measured intensity at each urea concentration and the average lifetime in the absence of urea. This average lifetime value in the absence of urea was taken to be the weighted sum of each of the components recovered from the analysis. These calculated values of average fluorescence lifetime vs [urea] were then used with the values of anisotropy as described under Materials and Methods to calculate the change in the average rotational correlation time as a function of urea concentration.

The results of this calculation are shown in Figure 7A. It is clear from these plots that both in the absence and in the presence of tryptophan, the urea denaturation profiles are biphasic. The decrease in the fluorescence lifetime at low urea concentration in the absence of tryptophan masks the changes in rotational properties between 0 and 4 M urea when only the anisotropy is considered. However, in the plot of the rotational correlation time, the decrease in the correlation time at low urea concentrations is seen. We interpret the low urea transition as arising from the dissociation of the residual repressor tetramers which are present at this concentration. In the presence of tryptophan, this low urea transition is complete by 2.5 M urea, whereas in the absence of co-repressor, the transition is more gradual and slightly overlaps with the main unfolding transition. This is consistent with the destabilization of repressor tetramers by tryptophan binding which we have previously reported (Fernando & Royer, 1992). Since the changes in local fluorophore motions upon tetramer dissociation are larger in the presence of co-repressor than in its absence, the value of the average rotational correlation time which corresponds to dimeric repressor is quite low in the presence of tryptophan. We have found the low urea transition to be sensitive to protein concentration, which supports the interpretation that this transition is due to tetramer dissociation. Plots of the correlation times of the DNS-labeled repressor in the absence and presence of tryptophan and at two protein concentrations each between 0 and 4 M urea are shown in Figure 8. At this salt concentration (10 mM), the repressor tetramer is destabilized with respect to the profiles in Figure 7 which were carried out in the absence of salt. For this reason, the low urea transition observed in the presence of tryptophan is complete by 2 M urea at 6.8 μM in DNS-labeled repressor, and there is almost no tetramer present in the presence of tryptophan at 1 μM in protein resulting in no detectable change in the correlation time with increasing urea concentration at this lower concentration. In the absence of tryptophan, the decrease in correlation time occurs across the entire range studied, and the curve is shifted

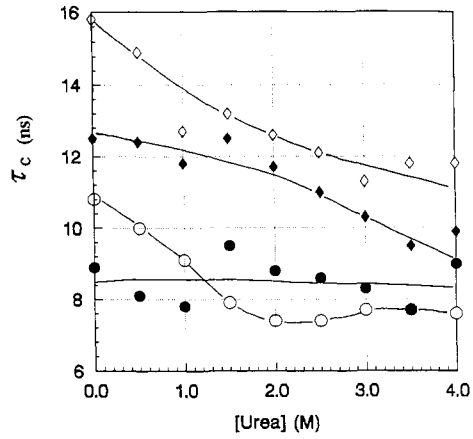

FIGURE 8: Concentration dependence of the low urea transition observed in the profiles of the average correlation times of the DNS-labeled repressor. (A) In the absence of tryptophan at 10 μM (◊) and 1.0 μM (♦) in DNS-labeled repressor dimer. (B) In the presence of 0.4 mM tryptophan at 6.8 μM (○) and 1.0 μM (●) in repressor dimer. Lines drawn through the data points are simply for clarity and do not represent any fit of the data.

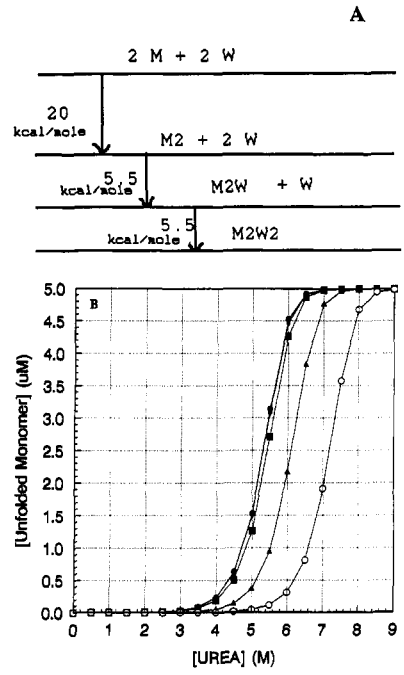

FIGURE 9: Simulations of 2.5 μM *trp* repressor dimer unfolding by urea in the presence of varying concentrations of tryptophan. (A) The free energy diagram used in the simulations. M is unliganded monomer, W is tryptophan, M_2 is unliganded dimer, M_2W is once-liganded dimer, and M_2W_2 is twice-liganded dimer. (B) Results of the simulations with 4 pM (●), 4 μM (♦), 40 μM (■) 400 μM (▲), and 4 mM (○) tryptophan. The degree of unfolding is presented as the concentration of unfolded, unliganded monomer.

to lower values of correlation time upon dilution from 10 to 1 μM in repressor due to a decrease in the amount of tetramer. As seen in Figure 7B, the midpoint of the main unfolding transition is found near 5.5 M urea in the absence of tryptophan and near 6.5 M urea in the presence of the co-repressor. In order to calculate the free energy of stabilization due to the presence of tryptophan, we fit the portions of the two curves in Figure 7A which corresponded to the main unfolding transition as described under Materials and Methods. In the absence of tryptophan, the low urea transition overlaps the main transition to some extent, but the transition beyond 4 M urea is fairly sharp. The use of part of the rotational correlation time profile obtained in the absence of co-repressor in order to fit the dimer to unfold monomer transition is justified by the fact that the DNS correlation time and the intrinsic tryptophan denaturation profiles are quite comparable in the range of the main transition. In Figure 7B, the DNS rotational correlation time data in the absence and presence of co-repressor are plotted along with the results of a nonlinear least-squares analysis of the data as described under Materials and Methods. It is evident from these data that the binding of tryptophan stabilizes the repressor against the main denaturation transition. This analysis yields a free energy of unfolding for the DNS-labeled aporepressor of 18.3 kcal/mol and 24.1 kcal/mol for the holorepressor. There is thus an apparent stabilization of 5.7 kcal/mol of the repressor dimer upon addition of 0.4 mM co-repressor. The results of these fits are summarized in Table I.

DISCUSSION

In the present studies, we have used fluorescence polarization to bring to light the urea-induced dissociation of oligomers of the *trp* repressor. None of the techniques used previously for *trp* repressor denaturation were sensitive to the dimer–tetramer equilibrium, and thus this transition was not resolved specifically, although the changes in NMR signals observed by Lane and Jardetsky (1987) at obviously very high concentrations may reflect oligomer dissociation. Since oligomer dissociation is essentially complete by 4 M urea, even in the absence of co-repressor, and since the intrinsic tryptophan intensity is insensitive to this transition, the CD, difference absorption, and fluorescence intensity data by Gittelman and Matthews (1990) as well as our own emission energy data are quite consistent with a simple dimer to unfolded monomer transition. The midpoints of the transitions which we observe are quite close to those reported by Gittelman and Matthews, although the extrapolated free energies are somewhat different. We find a free energy of 19.2 kcal/mol, compared to 22.4 kcal/mol reported by Gittelman and Matthews. However, given that the linearity assumption is merely an approximation and that even if correct the error on these determinations is between 1 and 2 kcal/mol, the agreement is quite reasonable. We have also determined that the addition of 0.4 mM in tryptophan results in an apparent stabilization of the dimer against denaturation of approximately 5.7 kcal/mol. As in the case of simple dimer dissociation, the degree of stabilization depends upon the absolute concentration of the stabilizing ligand. If we assume that either in the absence or in the presence of tryptophan the unfolding transition is concerted, then the relative chemical potentials of all of the possible species should vary in the same manner with the concentration of urea; that is, they should exhibit the same slope in eq 4. In order to simulate what effect the varying tryptophan concentrations should have upon the main transition of the dimer denaturation curve, we have adapted the numerically based binding data analysis program of Royer and co-workers (Royer et al., 1991) to simulate denaturation experiments. The free energies employed in the simulations are those given in the diagram given in Figure 9A. The transition from unliganded dimer to unfolded monomer was taken to be 20 kcal/mol. Given that these simulations were run for protein concentrations which are in the micromolar range, the existence of folded monomer at 0 M urea was not considered, and the only monomeric species assumed to be populated was the unfolded form. The free energy of tryptophan binding was assumed to be 5.5 kcal/mol (Joachimiak et al., 1983; Arvidson et al., 1986; Chou et al., 1991; Youderian, personal communication). A slope of 2.4 was used in the simulations for the [urea] dependence of all of the free energies. As can be seen from the results of the simulations

in Figure 9B, addition of 40 μM tryptophan (near the K_d) results in only a very small shift of the denaturation profile to higher urea concentrations. However, in the presence of 0.4 mM tryptophan (the concentration used in our studies), the curve is shifted by approximately 0.8 M urea. This simulates well the observed effect of tryptophan shown in Figure 7B. Addition of 4 mM tryptophan shifts the midpoint of the curve even further to near 7.2 M urea.

It is also worthwhile to consider briefly the energetics of the dimer denaturation/dissociation transition in the absence of tryptophan, assuming that the extrapolation assumption is a reasonable approximation. The total free energy of the transition from unliganded dimer to unfolded monomer in the absence of tryptophan is approximately 20 kcal/mol. We have shown previously that the repressor dimer in the absence of tryptophan will dissociate to monomer. We have estimated the K_d for this dissociation to be between 0.1 and 1 nM. Assuming the lowest value for the K_d, the free energy for dimer dissociation is near 14 kcal/mol. This leaves approximately 3 kcal/mol of stability for each monomer and suggests that upon dilution monomeric *trp* repressor retains a non-negligible degree of structural integrity.

We have demonstrated that upon denaturation by urea, the fluorescence lifetime continues to change, as does the intensity as reported by Gittelman and Matthews (1990) beyond the main structural transition. Given the structure of the repressor and the partial resolution of the fluorescence decays of the two tryptophan residues, it is not unreasonable to suggest that this observed increase in intensity at high urea concentrations arises in part from the alleviation of quenching of tryptophan-99 in the separated monomers. In the primary sequence, W99 is preceded by glutamine-98 and arginine-97. Both of these groups would be relatively efficient quenchers. The continued addition of urea beyond the concentration corresponding to the end of the main unfolding transition could reasonably lead to further penetration of the urea into the denatured monomers, resulting in a further separation of the quenching moieties from the W99 and therefore a continual increase in its fluorescence intensity. It is unlikely, although not impossible, that these secondary changes are a result of large rearrangements in the denatured state. Future studies of the denaturation of the single tryptophan mutants of the repressor will lead to further insight into the physical basis for the observed changes in the fluorescence emission properties upon denaturation.

Monitoring protein denaturation at equilibrium is essential for understanding the complex mechanisms of protein folding and stability. Clearly, most polypeptides undergo a concerted and very large change in their three-dimensional structure upon perturbation by heating or addition of chemical denaturants. This large concerted transition has been brought to light in a large number of proteins using physical techniques which include circular dichroism, fluorescence and NMR, among others. In the case of the *trp* repressor, Gittelman and Matthews (1990) demonstrated very good agreement between the transitions observed by CD, fluorescence intensity, and difference absorption measurements. Lane and Jardetsky (1987), however, demonstrated that different NMR signals yielded quite different denaturation profiles. It is important when interpreting the effect of a denaturing perturbation upon a physical observable to keep in mind the origin of the particular signal being followed. Circular dichroism, since it gives a measure of the average amount of secondary structure in the protein, is quite suitable for detecting the denaturation transition which is responsible for the major loss of structure. The other spectroscopic techniques, UV absorption, fluorescence, and nuclear magnetic resonance, report on changes in the local environment around the probe giving rise to a particular signal. While the main structural transition will likely cause an observable perturbation in these spectroscopic parameters, it is also possible that these methodologies will report rather large changes that are, in fact, due to rather small-scale local rearrangements.

The instrumentation and analysis methodologies used for probing solution structures and dynamics of macromolecules are becoming increasingly more sophisticated. This has resulted in the ability to at least partially resolve heterogeneous populations of protein molecules. Clearly, perturbing the protein solution with chemical denaturants or temperature results in an increase in the heterogeneity of these populations. Depending upon the techniques which one employs, different aspects and areas of the global structure and dynamics are probed, and varying degrees of detail are achieved. Comparisons, therefore, of experimental results obtained with multiple techniques should give weight to the nature of the physical observables and their probable relation to structure. Fluorescence spectroscopic methods, particularly time-resolved approaches, for monitoring denaturation processes present the advantage of being exquisitely sensitive to changes in the structure, dynamics, and polarity of the environment. This sensitivity usually gives rise to a very large change in the observable fluorescence signal (color intensity, lifetime, rotational rate) upon unfolding of the protein. Moreover, fluorescence experiments can be carried out over a broad range of protein concentrations which coincides well with the concentration range for a number of protein–protein interactions. Additional structural or dynamic rearrangements are also often observed, either preceding or following the main unfolding transition, particularly if time-resolved experiments are performed. The difficulty then lies in the interpretation of these secondary changes. In general, they are ignored, and the main unfolding parameters are obtained from the fluorescence data corrected for any secondary effects. Detailed investigation of these secondary changes could yield information concerning the structure of the denatured state, the nature of intermediates, and the effect of the perturbant upon these species.

It is also worthwhile to point out that each individual protein will exhibit a characteristic fluorescence response to unfolding. For example, the fluorescence intensity of the *trp* repressor increases considerably upon unfolding, while that of staphylococcal nuclease becomes quenched by approximately 70% (Shortle, 1986). The absolute values of the average lifetimes of the fluorophores in the denatured states of these proteins are respectively higher and lower than that of *N*-acetyltryptophanamide in water. These observations imply that there is a distinct structure for each of these proteins in the denatured state and that the tryptophan emission is not that of a random-coil, completely solvent-exposed moiety. There are clearly subtleties in the detection of folding intermediates as well as in assessing their importance in determining protein structure and stability. Time-resolved and steady-state fluorescence spectroscopy, with its multiple observable parameters, will surely yield a great deal of information concerning the existence of folding intermediates in a number of protein systems. Likewise, consideration of observed fluorescence changes in light of the known primary, secondary, and tertiary structures for well-studied proteins will likely aid in building a framework for the interpretation of the fluorescence properties of less well-characterized systems.

ACKNOWLEDGMENT

Some of the data were obtained at the Laboratory for Fluorescence Dynamics, which is a national research center jointly funded by the National Institutes of Health and the University of Illinois at Urbana—Champaign. We also thank Dr. Kathleen Shive Matthews for the plasmid and bacterial strain used to overproduce the repressor protein. We are also grateful to Ronit Spotts and Yuan Ching Liu, of the K. S. Matthews laboratory, for providing much of the protein used in these studies, for carrying out the gel mobility shift assays, and for their advice in protein purification. Dr. Hans Liao of the Biotechnology Center of the University of Wisconsin—Madison graciously offered his assistance in transforming and growing the overproducing strain.

REFERENCES

Arvidson, D. A., Bruce, C., & Gunsalus, R. P. (1986) *J. Biol. Chem. 261*, 238–243.

Beechem, J. M., Gratton, E., Ameloot, M., Knutson, J. R., & Brand, L. (1992) in *Fluorescence Spectroscopy: Principles and Techniques*, (Lakowicz, J. R., Ed.) Vol. I, Plenum Press, New York.

Carey, J. (1988) *Proc. Natl. Acad. Sci. U.S.A. 85*, 975–979.

Chou, W.-Y., & Matthews, K. S. (1989) *J. Biol. Chem. 264*, 18314–18319.

Fernando, T., & Royer, C. A. (1992) *Biochemistry 31*, 3429–3441.

Guest, C. R., Hochstrasser, R. A., Dupuy, C. G., Allen, D. J., Benkovic, S. J., & Millar, D. P. (1991) *Biochemistry 30*, 8759–8770.

Gittelman, M. S., & Matthews, C. R. (1990) *Biochemistry 29*, 7011–7020.

He, J.-J., & Matthews, K. S. (1989) *J. Biol. Chem. 265*, 731–737.

Jameson, D. M. (1978) Ph.D. Dissertation, University of Illinois, Urbana, IL.

Joachimiak, A., Kelley, R. L., Gunsalus, R. P., Yanofsky, C., & Sigler, P. B. (1983) *Proc. Natl. Acad. Sci. U.S.A. 80*, 668–672.

Kumamoto, A. A., Millar, W. G., & Gunsalus, R. P. (1987) *Genes Dev. 1*, 556–564.

Lambooy, P. K., Steiner, R. F., & Sternberg, H. (1982) *Arch. Biochem. Biophys. 217*, 517–528.

Lane, A. N., & Jardetsky, O. (1987) *Eur. J. Biochem. 164*, 389–396.

Otwinowski, Z., Schevitz, R. W., Zhang, R.-G., Lawson, C. L., Joachimiak, A., Marmorstein, R. Q., Luisi, B. F., & Sigler, P. B. (1988) *Science 335*, 321–329.

Pace, N. C. (1986) *Methods Enzymol. 131*, 266–280.

Paluh, J. L., & Yanofsky, C. (1986) *Nucleic Acids Res. 14*, 7851–7860.

Piston, D. W., Marriott, G., Radiveyovich, T., Clegg, R. M., Jovin, T. M., & Gratton, E. (1989) *Rev. Sci. Instrum. 60*, 2596–2600.

Royer, C. A., Rusch, R. M., & Scarlata, S. F. (1989) *Biochemistry 28*, 6631–6637.

Royer, C. A., Chakerian, A. E., & Matthews, K. S. (1990) *Biochemistry 29*, 4959–4966.

Royer, C. A., Smith, W. R., & Beechem, J. M. (1991) *Anal. Biochem. 191*, 287–294.

Schevitz, R. W., Otwinowski, Z., Joachimiak, A., Lawson, C. L., & Sigler, P. B. (1985) *Nature 317*, 782–786.

Shortle, D. (1986) *J. Cell. Biochem. 30*, 281–289.

Shortle, D., Meeker, A. K., & Gerring, S. L. (1989) *Arch. Biochem. Biophys. 272*, 103–113.

Staake, D., Walter, B., Kissers-Woike, B., von Wilcken-Bergmann, B., & Muller-Hill, B. (1990) *EMBO J. 9*, 1963–1967.

Zhang, R., Joachimiak, A., Lawson, C. L., Schevitz, R. W., Otwinowski, Z., & Sigler, P. B. (1987) *Nature 327*, 591–597.

Registry No. Trp, 73-22-3; urea, 57-13-6.